ON THE FORMULATION OF GENERAL SHELL ELEMENTS USING MIXED INTERPOLATION OF TENSORIAL COMPONENTS

Eduardo N. Dvorkin

Dalmine Siderca and Instituto de Materiales y Estructuras.
Facultad de Ingeniería. Universidad de Buenos Aires.
Buenos Aires - Argentina.

RESUMEN

En esta comunicación resumimos brevemente nuestras investigaciones sobre formulación de elementos de lámina no-lineales.

Empezamos definiendo los requerimientos que nos hemos fijado para desarrollar elementos de lámina y presentando nuestro método para satisfacer dichos requerimientos. Finalmente comentamos sobre algunos aspectos prácticos de la implementación de elementos de lámina.

ABSTRACT

In this communication we briefly review our research in the field of general nonlinear shell elements formulation.

We begin by defining the requirements we have set upon our development of shell elements, and presenting our approach to meet those requirements. Finally we comment on some practical aspects of the implementation of nonlinear shell elements.

1. INTRODUCTION

The development of shell elements has been a very active research field for the last two decades [1]. Many elements have been proposed, and the advances have been impressive, but shell analysis is still not a field where a finite element code can be always used in a routine way. In nonlinear analysis the need of expert use of the available shell elements and the limitations of the available shell analysis capabilities are even larger.

Therefore there is still need for research towards the develop - ment of reliable analysis capabilities.

It is here important to point out that according to our experience a very successful plate element can lead to an unsuccessful shell ele - ment and in the same way a very successful linear shell element can lead to an unsuccessful nonlinear shell element.

It is, therefore, of advantage to concentrate directly on the deve- lopment of general nonlinear shell elements, which can afterwards be specialized to obtain linear shell elements and plate elements.

The requirements we have set upon our development of shell elements [2-7] are governed by our desire to render this elements widely applica- ble in routine analyses (e.g. CAD situations). For this purpose an ele - ment should ideally satisfy the following criteria [7]:

Criterion 1: The element should be formulated as general as possible, to be applicable in any plate/shell situation.

Criterion 2: The theoretical formulation of the element should be strongly continuum mechanics based, with assumptions in the finite ele - ment discretization that are mechanistically clear and well founded.

Criterion 3: The element should not contain any spurious zero energy mode and should not lock under any condition. Also it should not contain numerically adjusted factors.

Criterion 4: The element should be simple and inexpensive to use with, for shell analyses, five or six engineering degrees of freedom per node, and for plate analyses the three engineering degrees of free- dom per node.

Condition 5: The predictive capability of the element should be high and relatively insensitive to element distortions.

The criteria summarized above are the basis of a reliable and effec tive shell element. We strongly believe that the reliability of an ele - ment is of utmost concern and is, for example, much more important than its cost/effectiveness.

To construct our new shell elements based on the mixed interpola - tion of tensorial components [4-7], we have used our accumulated in- sight into the behavior of elements, to satisfy the elements require- ments we stated above as closely as possible.

As a basic tool to test our developments we used Iron's patch test [9] as a first filter, and afterwards we measured the order of convergence of our elements by solving some well-established problems.

For performing the patch tests, we subject the patch of elements (see Figs. 4 and 9) to nodal point displacement constraints just sufficient to remove all physical rigid body modes, and to externally applied boundary nodal point forces that correspond to constant boundary stress conditions. The analysis yields the nodal point displacements and the internal element stresses. The patch test is passed if those predicted quantities correspond to the analytical solution.

For our 4-node element a variational formulation was proposed in references [4-5], which corresponds to a particular application of the Hu-Washizu variational principle [10]. Also a formal convergence study was carried out for some specific cases in reference [11].

Recently our approach was used by Huang and Hinton [12].

Related approaches are being investigated by Crisfield [13] and Park and Stanley [14].

2. THE AHMAD ELEMENT

Perhaps the most general shell element now available is the degenerate isoparametric shell element presented first for linear analysis by Ahmad, Irons and Zienkiewicz [15]. Among others Ramm [16] and Bathe and Bolourchi [3,17] developed the Ahmad element for nonlinear analysis.

This element presents the basic problem of shear locking [8,17] and, in curved elements, also membrane locking [18].

To illustrate the locking phenomena we will consider beam elements formulated by means of the Ahmad, Irons and Zienkiewicz formulation (Timoshenko beams) [17]. It is important to point out that although the beam examples can illustrate on the locking phenomena, the analysis of locking in shell elements is much more involved, and also to formulate shell elements that do not lock is much more involved than to formulate beam elements that do not lock.

2.1 Shear locking in the Ahmad elements

For the 2-node cantilever beam of Fig. 1, the functional of the total potential energy is:

$$\pi = \frac{EI}{2} \left[\int_0^L (\theta_{,1})^2 \, dx_1 + \alpha \int_0^L [\frac{1}{L}(u_{3,1} - \theta)]^2 dx_1 \right] \quad (1)$$

where,

$$\alpha = \frac{12\, G\, k}{E} \left(\frac{L}{h}\right)^2$$

$$- M\theta^2$$

In the above $I = bh^3/12$ and k is the shear correction factor [17].

It is evident from (1) that $\alpha \longrightarrow \infty$ when $h/L \longrightarrow 0$, i.e. when the beam element is very thin, the second term in the r.h.s. acts as a penalty to impose the condition.

$$\gamma = u_{2,1} - \theta = 0 \tag{2}$$

If we impose the rotations corresponding to a constant curvature of the beam, the satisfaction of Eqn. (2) at the 2 Gauss integration points on the beam axis, leads to,

$$\frac{u_2^1}{L} - \frac{1}{2}\left(1 + \frac{1}{\sqrt{3}}\right)\theta^2 = 0$$

$$\frac{u_2^2}{L} - \frac{1}{2}\left(1 - \frac{1}{\sqrt{3}}\right)\theta^2 = 0 \tag{3.a}$$

The only way Eqs. (3.a) can be satisfied is if $u_2^1 = \theta^2 = 0$ (locking).

In effect, using (1) and invoking $\delta\Pi = 0$, we get [4],

$$\frac{\theta_{FEM}^2}{\theta_{AN.}^2} = \frac{1}{1 + \dfrac{Gk}{E}\left(\dfrac{L}{h}\right)^2} \tag{3.b}$$

which shows that for very thin elements, $(L/h) \longrightarrow \infty$, $(\theta_{FEM}^2/\theta_{AN.}^2) \longrightarrow 0$.

The locking problem appears because $\gamma \cong 0$ cannot be represented by the trial functions that span the finite element solution space.

2.2 Membrane locking in curved Ahmad elements

For a circular cantilever beam, under a constant bending moment, the functional of the total potential energy is:

$$\Pi = \frac{EI}{2}\left[\int_0^L \theta_{,1}^2 \, ds + \alpha_M \int_0^L u_{s,s}^2 \, ds \right.$$

$$\left. + \alpha_s \int_0^L (u_{n,s} - \theta)^2 \, ds\right] - M\theta^2 \tag{4}$$
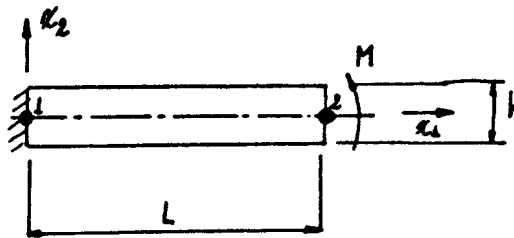
u_i^k : displacement of node K in the i-direction.

θ^k : rotation of node K.

E : Young's modulus.

G : shear modulus.

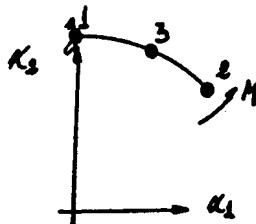b : width of the beam.

Figure 1. Cantilever under constant bending.

Figure 2.a Curved cantilever under constant bending.

R = 20
h (thickness) = 0.2
E = 2.1 x 10^6
v = 0.3
Int = 4x4x2

α	θ_{FE}/θ_{TH}
30°	0.02
20°	0.09
10°	0.62
5°	0.96

3 x 10° elements θ_{FE}/θ_{TH} = 0.61
6 x 5° elements θ_{FE}/θ_{TH} = 0.96

R = 20
h (thickness) = 0.2
E = 2.1 x 10^6
v = 0.3
Int = 4x4x2

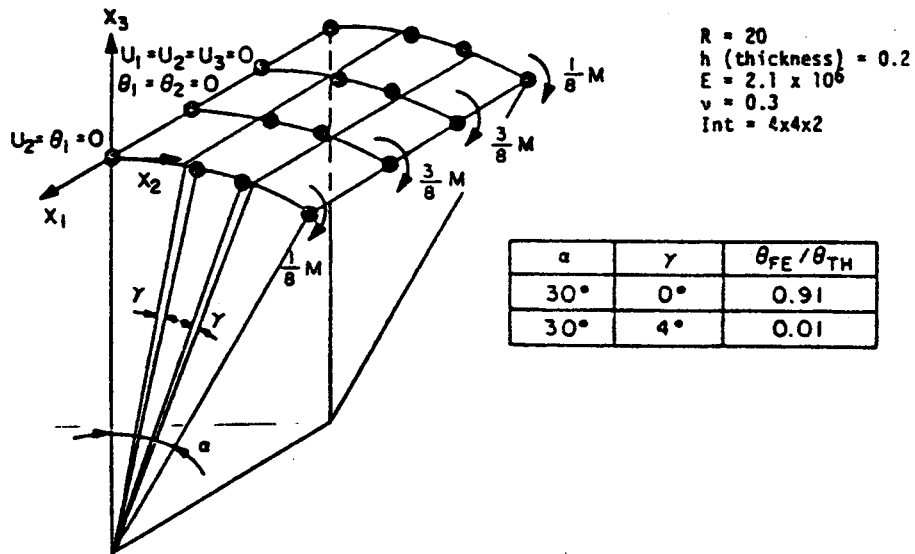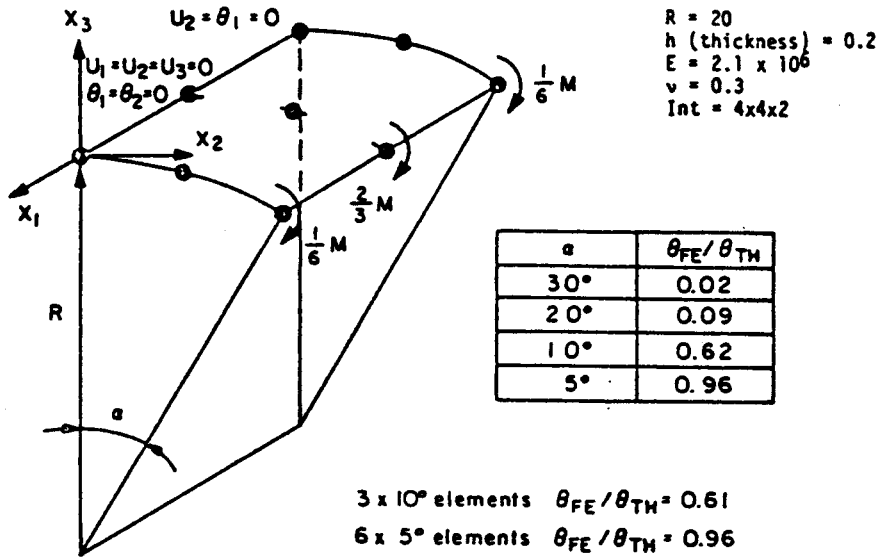| α	γ	θ_{FE}/θ_{TH}
30°	0°	0.91
30°	4°	0.01

Figure 2.b   Analysis of curved cantilever model
(Note that the figure is not to scale)

where L is the length of the circular beam measured along its axis, the Δ- direction is tangential to its axis and the η- direction is normal to its axis.

Since $\alpha_M = 12/h^2$ and $\alpha_\theta = 12Gk/h^2$; it is evident that when the beam becomes very thin, the second and third integrals in the r.h.s. act as a penalty to impose the conditions

$$\mathcal{E}_{\Delta,\Delta} = \mathcal{U}_{\Delta,\Delta} \equiv 0 \qquad (5.a)$$

and, $$\gamma_{\eta,\Delta} = \mathcal{U}_{\eta,\Delta} - \theta \equiv 0 \qquad (5.b)$$

that is to say zero membrane strains and zero transverse shears.

In the 3-node iso-beam of Fig. 2, let us prescribe the rotations θ^i (i = 1,2,3) corresponding to the analytical solution and from imposing Eqs. (5.a) and (5.b) at the 3 Gauss integration points we obtain a system of 6 equations with 4 unknowns $\mathcal{U}_i^k$; $k=1,3$; $i=1,2,3$ which cannot be solved, demonstrating the combined shear/membrane locking.

If the shear locking is removed, by interpolating the transverse shear strain through two points, we still have 5 equations and 4 unknowns, which cannot be solved, demonstrating the membrane locking.

In Fig.2.b we show some results corresponding to the analysis of a curved cantilever using the Ahmad shell element where the locking effect is displayed [4,8].

2.3 Remedies for the locking problem

It has been observed that when the finite element matrices are calculated using either uniform reduced numerical integration or selective reduced numerical integration [19], the locking problem is removed, but most of the times spurious zero energy modes are introduced at the element level (in shell elements).

This spurious zero energy modes are a not desirable characteristic specially in nonlinear analysis [4].

Therefore, another way of overcoming the locking problem is necessary, a more controlled approach that does not introduce undesirable features in the element.

3. OUR FOUR NODE ELEMENT BASED ON MIXED INTERPOLATION OF TENSORIAL COMPONENTS

3.1 Formulation of the element

The element reviewed in this section has been presented in detail in references [4-7].

Our 4-node element is based on the Ahmad degenerate element, the bending and membrane strains are calculated as usual from the displacement interpolations, while the transverse shear strains are interpolated differently.

Related approaches were used by MacNeal [20] and Hughes and Tezduyar [21] to develop linear plate elements and Wempner et al [22] to develop a shell element. Figure 3 shows a schematic view of the shell element and the nodal point degrees of freedom, it also shows the transverse shear strain interpolations.

$$\tilde{\mathcal{E}}_{13} = 1/2 \left(1 + r_2\right) \left.\tilde{\mathcal{E}}_{13}\right|_A^{DI} + 1/2 \left(1 - r_2\right) \left.\tilde{\mathcal{E}}_{13}\right|_C^{DI}$$

$$\tilde{\mathcal{E}}_{23} = 1/2 \left(1 + r_1\right) \left.\tilde{\mathcal{E}}_{23}\right|_D^{DI} + 1/2 \left(1 - r_1\right) \left.\tilde{\mathcal{E}}_{23}\right|_B^{DI} \qquad (6)$$

In (6), to allow for non-flat elements we interpolate the covariant components of the strain tensor, measured in the convected coordinate system of the element.

In (6), the variables $\left.\tilde{\mathcal{E}}_{ij}\right|_{A,B,C,D}^{DI}$ are the strain components at points A, B, C, D directly evaluated from the displacements interpolations. In our notation the superscript DI always signifies "direct interpolation from nodal point displacements and rotations". Therefore these variables are eliminated from Eq. (6), by expressing them in terms of the nodal point degrees of freedom.

Using the convected coordinate system, the governing finite element equations for time (load level) $t + \Delta t$ are derived using the principle of virtual work [17],

$$\int_{\sigma_V} {}_{\sigma}^{t+\Delta t}\tilde{S}^{ij} \, \delta \, {}_{\sigma}^{t+\Delta t}\tilde{\mathcal{E}}_{ij} \, {}^{\sigma}dV = {}^{t+\Delta t}R_\varphi \qquad (7)$$

where the ${}_{\sigma}^{t+\Delta t}S^{ij}$ are the contravariant components of the 2nd. Piola-Kirchhoff stress tensor and the ${}_{\sigma}^{t+\Delta t}\mathcal{E}_{ij}$ are the covariant components of the Green-Lagrange strain tensor, the integration is performed over the original volume, ${}^{\sigma}V$, of the element and ${}^{t+\Delta t}R_\varphi$ is the total external virtual work.

The following observations can be made about the element:

. The presented element is a general nonlinear shell element (the total lagrangian formulation [17] was used in its implementation), with the only restriction of small strains. Linear shell elements and plate elements can be obtained as particular cases.
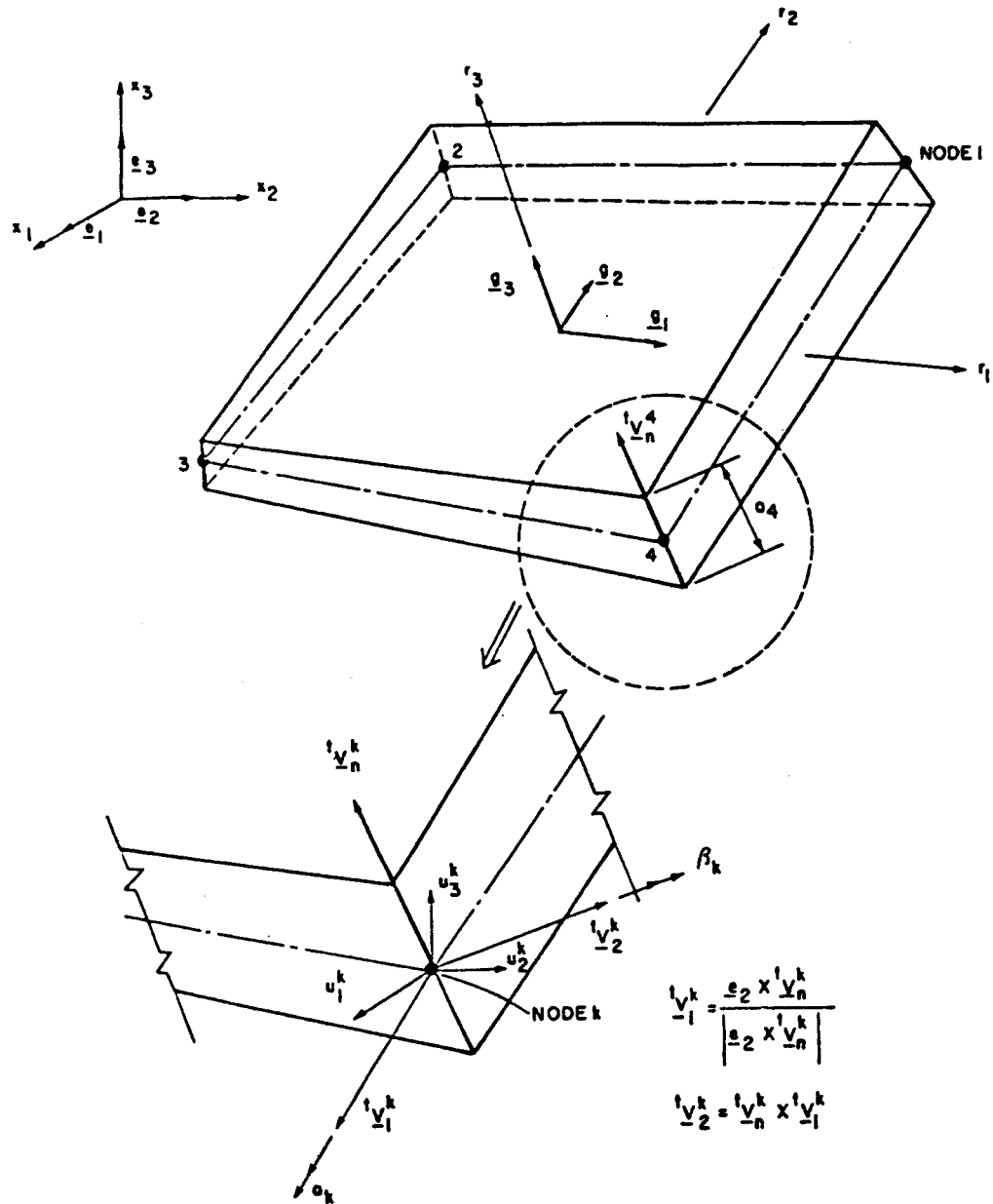
a) Element description

Figure 3 Four-node shell element

$\widetilde{\mathcal{E}}_{13}$ INTERPOLATION
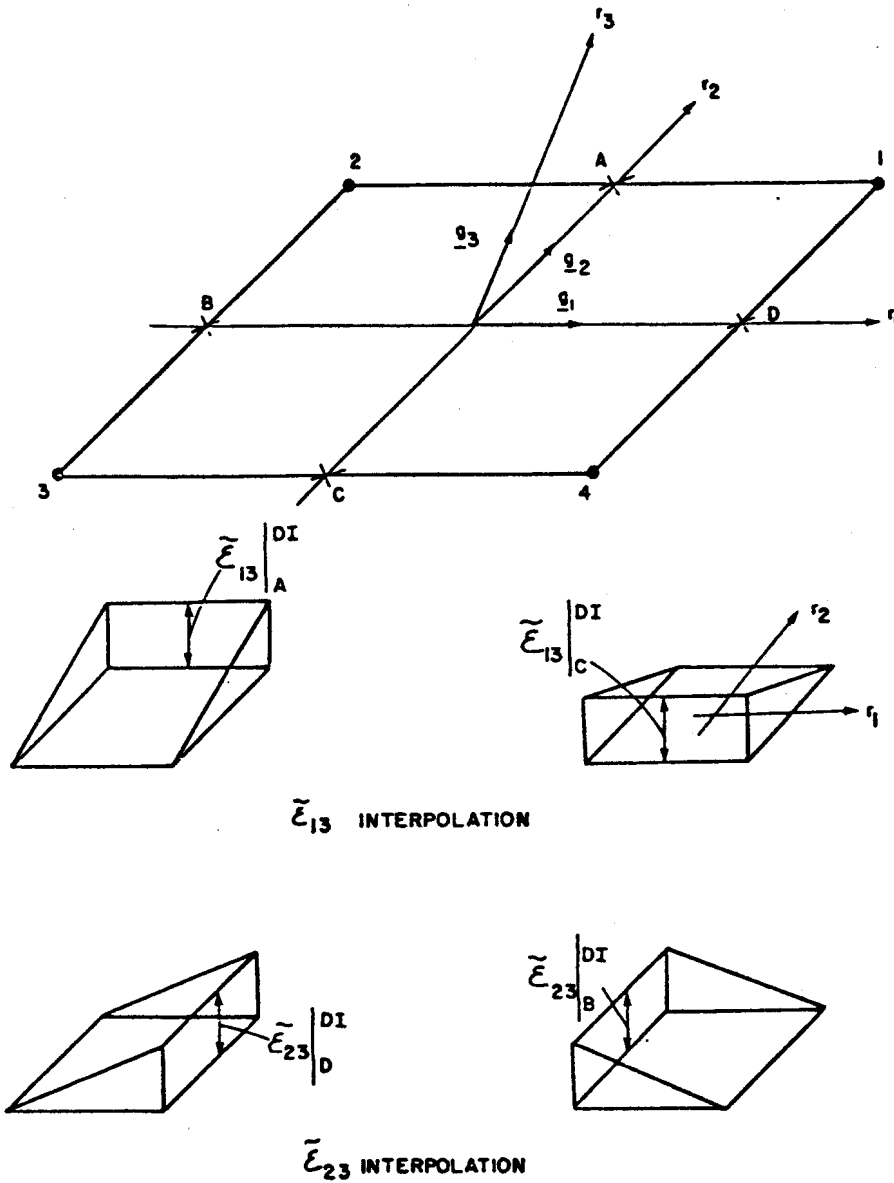
$\widetilde{\mathcal{E}}_{23}$ INTERPOLATION

b) Transverse shear strain interpolation functions

Figure 3 continued

. The element does not lock, does not contain spurious zero energy modes and is quite insensitive to elements distortions.

. Gauss integration is used to evaluate the element matrices, 2 x 2 integration is used in the mid-surface of the element, for linear elastic material 2 points are also used through the thickness, in plate elements the integration through the thickness is analytically performed [6].

For nonlinear material models accuracy considerations may lead to the use of more integration points.

3.2 Verification of the element.

3.2.1 The patch test.

As we stated in section 1, the first step in the verification of an element is to show that the element satisfies the different patch tests (membrane patch tests, bending patch tests, etc.).

In references [4-6] we presented numerical examples showing that our element satisfies the patch tests shown in Fig. 4, being the membrane patch tests obviously satisfied.

In reference [7] we presented an analytical proof that the bending patch test is passed. The derivation of that analytical proof apart from reinforcing our understanding of the element, also yields insight on how to construct higher order elements that satisfy the patch test.

3.2.2 Some numerical experimentation

In references [4-6] we presented an organized numerical investigation of the element, showing that,

I. The element does not have spurious zero energy modes and passes the patch test (the element is consistent [23]).

II. The element can approximate the Kirchhoff-Love hypothesis for thin shells (no locking).

III. The element has good convergence in the usual benchmark problems, and is quite insensitive to elements distortions.

IV. The elements has good behavior in some simple nonlinear problems.

V. The element has good predictive capabilities in some complicated nonlinear problems.

In this communication we will only show a few results to illustrate on the behavior of our element, MITC4 (for mixed interpolation of tensorial components with 4 nodes).

In Fig. 5 we present the analysis of a simply supported circular plate (radius/thickness = 10), subjected to a constant temperature gradient through the thickness (linear analysis). The results of the MITC4 element are compared with the results of the original degenerate element.
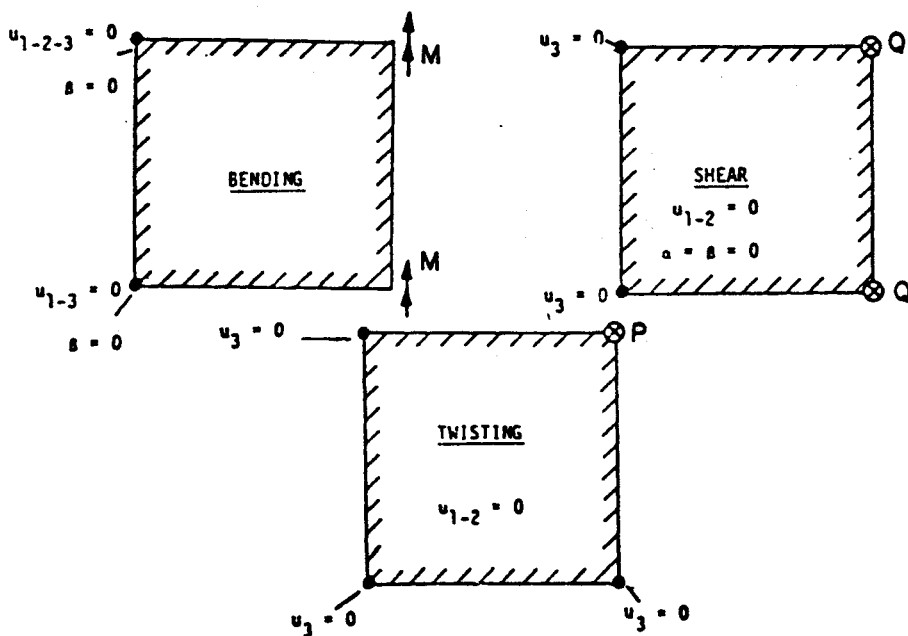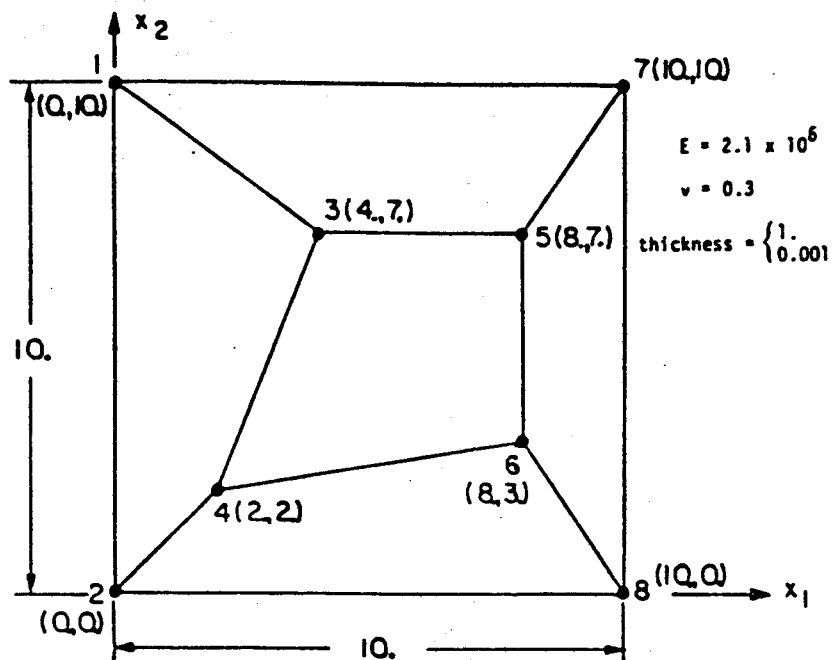
Figure 4   Patch tests

	F. E. M. MODEL	$\|\varepsilon_w\|\dfrac{\|W_{FE} - W_{anl}\|}{\|W_{anl}\|}$	ε_τ
Standard Isoparametric Element		-0.26	1.0
		-0.07	0.54
	INT. 3×3×2	-0.008	0.62 Central elem.
			0.22 Outer elem.
	SAME MODEL INT. 2×2×2	+0.014	0.02
	IN T. 4×4×2	-0.003	0.26
	SAME MODEL INT. 3×3×2	+0.0001	0.04
MITC4	INT. 2×2×2	0.0	0.0

Figure 5   Circular plate with constant temperature gradient through the thickness

$$\eta_b = \frac{\tau_{bending}^{max}}{\frac{3P}{h^2}}$$

$E = 1 \cdot 10^7$
$\nu = 0.3$
$L = 100$
$a = 2$
thickness $(h) = 1$
$P = 5$

SOLUTION	η_b at A
ANALYTICAL	1.576
MITC4	1.546

MESH

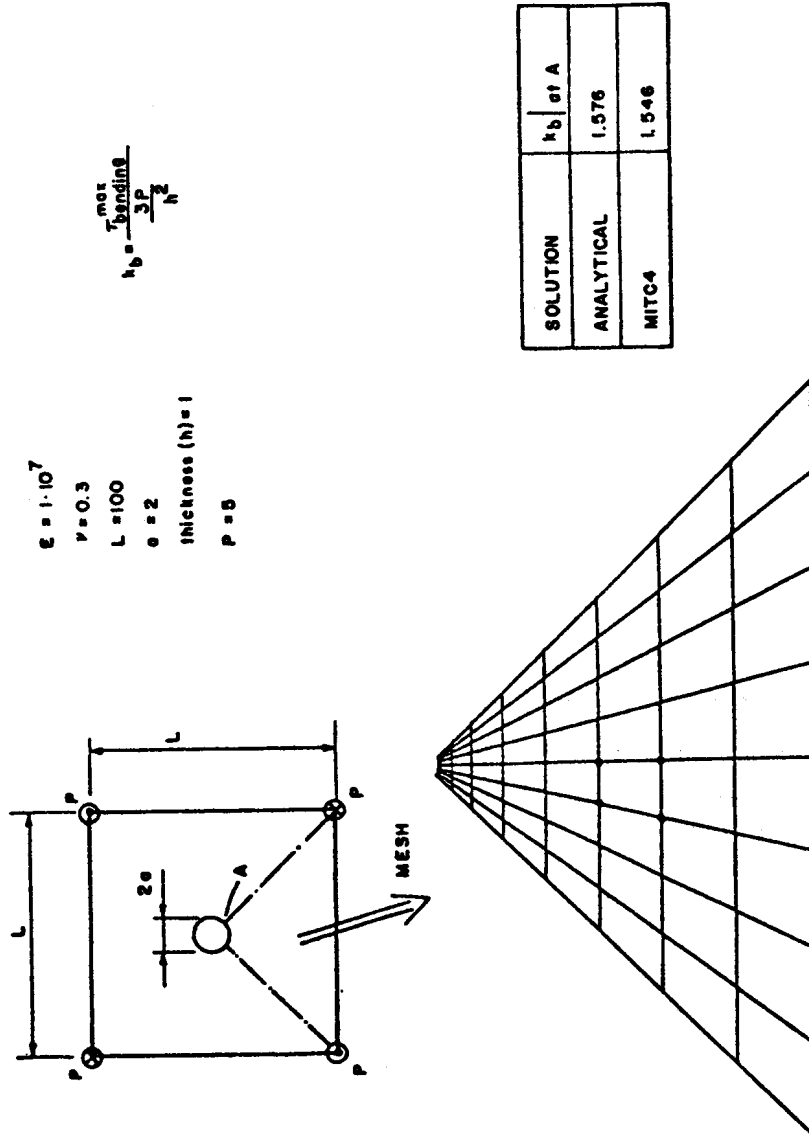Figure 6 Analysis of a plate with a hole under transverse twisting using the MITC4 element. The stresses are directly calculated at point A.

In the figure ϵ_T represents the relation between the maximum absolute value of principal stress predicted by the model and $(E \propto \theta)$ (being θ the temperature at the point and $\propto$ the thermal expansion coefficient). In the analytical solution $\epsilon_T \neq 0$.

This problem can be regarded as another way of presenting the bending patch test.

In Fig. 6 we show the analysis of a plate with a hole in twisting, the finite element solution is compared with the analytical solution presented in [24].

In Fig. 7 we consider the large displacement elastoplastic collap se response of a shell. The loading on the shell is uniform vertical pressure loading per unit of projected area on the horizontal plane. The solution is compared with the response predicted by Kråkeland [25], who solved for the response up to $W_a = 125$. . To obtain the solution we used the automatic load incrementation algorithm of ref. [26].

4. OUR EIGHT NODE ELEMENT BASED ON THE MIXED INTERPOLATION OF TENSORIAL COMPONENTS

4.1 Formulation of the element

The element reviewed in this section has been presented in detail in ref. [7].

The concept used to develop the 4-node element opens various possi bilities to develop effective higher-order curved shell elements, which we expect to present better convergence behavior in the displacements and stresses.

In studying various possible interpolations analytically and nume- rically we identified that the 8-node element described below offers much promise, see Fig. 8. At each nodal point, the same kinematic des- cription using director vectors and 5 degrees of freedom per node, as for the Ahmad element [17] and the MITC4 element, is used. Hence, the displacements are interpolated as usual [17].

To avoid shear and membrane locking we interpolate the in-layer strains and transverse shear strains independently - with appropriately selected interpolations - ant tie the coefficients in these interpola- tions to the strain components evaluated directly from the displacement field. The in-layer strain interpolation yields the membrane and bending action of the element, and the transverse shear strains interpolation gives the transverse shear action. To formulate the general shell element we interpolate the strain tensor expressed in terms of covariant tensor components $\mathcal{E}_{ij}$ and contravariant base vectors g^i measured in the convected system of the element.

In the following discussion we consider the element strain tensor at any time during the response history. However, for the incremental formulation we refer to [4,5, 17] and here we do not include the left superscript denoting time (e.g. $g_i \equiv {}^t g_i$). Also, we use the nota- tion $g_r = g_1$; $g_s = g_2$; $g_t = g_3$

E = 21,000

$\nu = 0$

$E_T = 0$

$\sigma_y = 4.2$

L = 15,200

R = 7,600

$\phi = 40°$

thickness = 76

RIGID DIAPHRAGM

9 X 9 UNIFORM MESH USED
TO REPRESENT AREA ABCD

$p \times 10^3$

O Krökeland

— MITC4

4 POINT GAUSS INTEGRATION
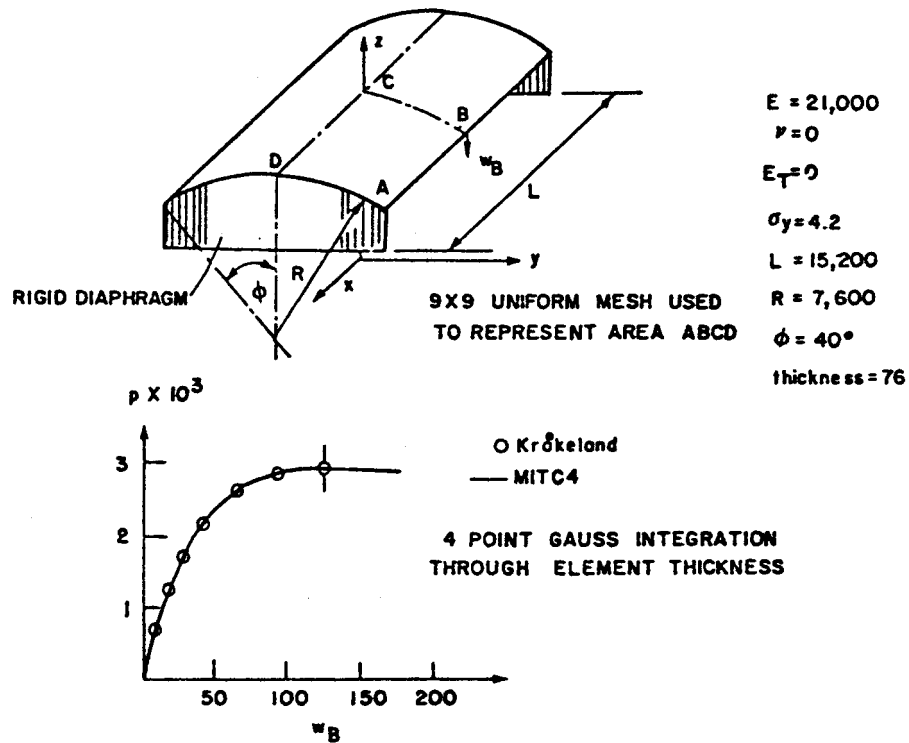THROUGH ELEMENT THICKNESS

w_B

Figure 7   Large deflection elastic-plastic analysis of a
cylindrical shell using the MITC4 element; p is
the vertical pressure per unit of projected area
on the horizontal plane.
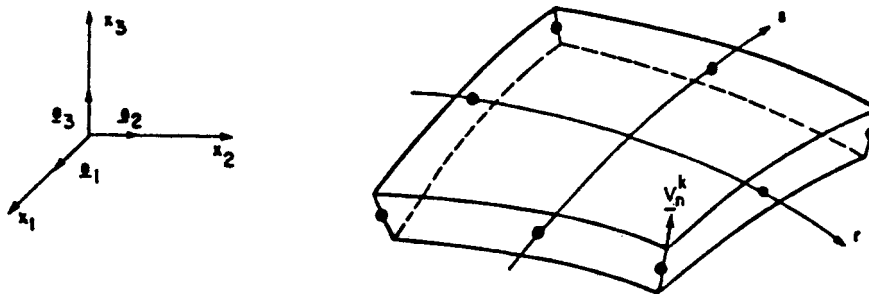
a) Element geometry
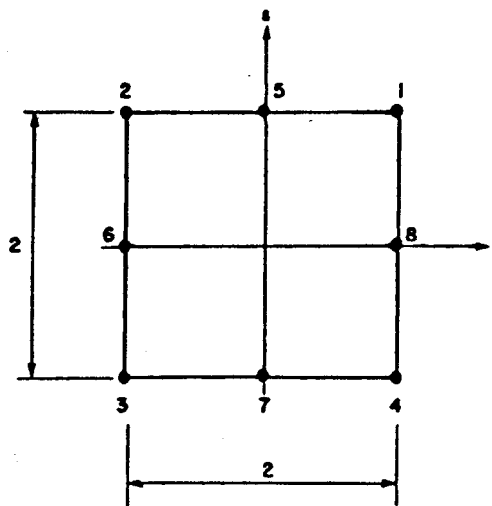
b) Nodes used for interpolation of displacements and rotations

Figure 8 Eight-node shell element
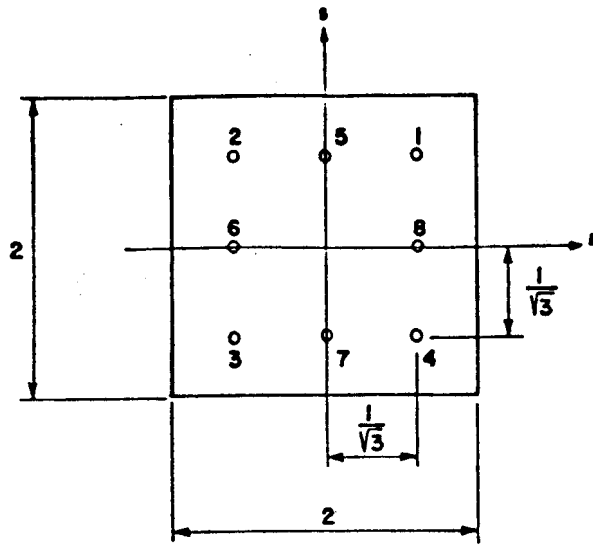
c) Points used for interpolation of in-layer strains
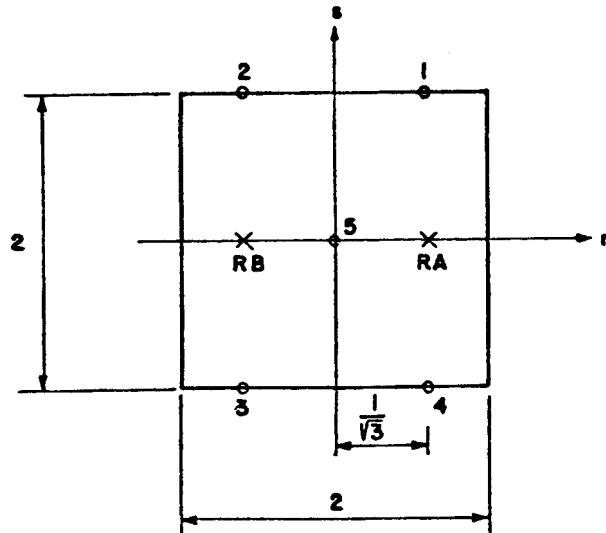
d) Points used for interpolation of transverse shear strain $\tilde{\varepsilon}_{rt}$ $\underline{g}^r$ $\underline{g}^t$

Figure 8 continued

e) Points used for interpolation of transverse shear strain $\tilde{\varepsilon}_{st}\ \underline{g}^s\ \underline{g}^t$

Figure 8 continued

The strain tensor at any point inside the element is:
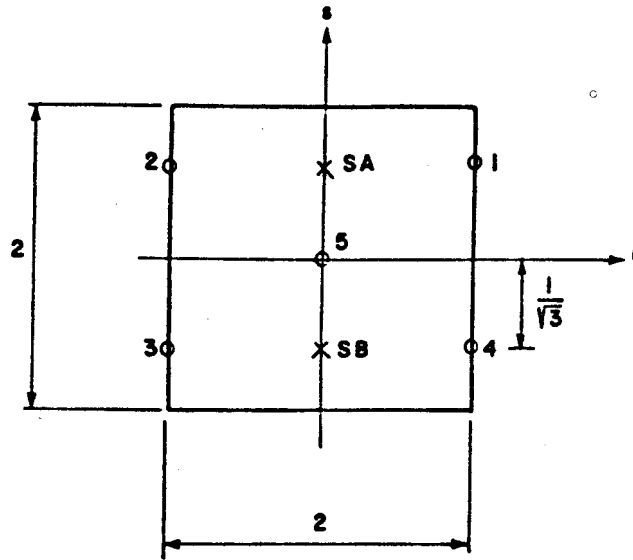
$$\underline{\mathcal{E}} = \underbrace{\tilde{\mathcal{E}}_{rr}\, \underline{g}^r \underline{g}^r + \tilde{\mathcal{E}}_{\Lambda\Lambda}\, \underline{g}^\Lambda \underline{g}^\Lambda + \tilde{\mathcal{E}}_{r\Lambda}\, (\underline{g}^r \underline{g}^\Lambda + \underline{g}^\Lambda \underline{g}^r)}_{\text{in-layer strains}} \tag{8}$$

$$+ \underbrace{\tilde{\mathcal{E}}_{rt}\, (\underline{g}^r \underline{g}^t + \underline{g}^t \underline{g}^r) + \tilde{\mathcal{E}}_{\Lambda t}\, (\underline{g}^\Lambda \underline{g}^t + \underline{g}^t \underline{g}^\Lambda)}_{\text{transverse shear strains}}$$

It must be taken into account that the hypothesis of constant thickness along the director vectors, on which the element is constructed, implies $\mathcal{E}_{tt} = 0$ [4,5].

The appropiate interpolation of the in-layer strains and of the transverse shear strains to satisfy our shell element requirements as closely as possible is the key aspect of our formulation.

To have no spurious zero energy modes, pass the patch test and avoid locking we use the following interpolations:

. In-layer strains, (see Fig. 8-c)

$$\underline{\mathcal{E}} = \sum_{i=1}^{8} h_i^{IS}\, \underline{\mathcal{E}}\big|_i \tag{9}$$

where the h_i^{IS} are obtained from the usual serendipitic interpolation functions of the 8-node element [17, Fig. 5.5], by replacing the variable r with r/a, and the variable Λ with Λ/a ; $a = 1/\sqrt{3}$.

Also, we have for i = 1, 2, 3, 4

$$\underline{\mathcal{E}}\big|_i = \tilde{\mathcal{E}}_{rr}\, \underline{g}^r \underline{g}^r \Big|_i^{DI} + \tilde{\mathcal{E}}_{\Lambda\Lambda}\, \underline{g}^\Lambda \underline{g}^\Lambda \Big|_i^{DI} + \tilde{\mathcal{E}}_{r\Lambda}\, (\underline{g}^r \underline{g}^\Lambda + \underline{g}^\Lambda \underline{g}^r)\Big|_i^{DI} \tag{10}$$

For i = 5 and 7

$$\underline{\mathcal{E}}\big|_5 = \tilde{\mathcal{E}}_{\Lambda}\, \underline{g}^\Lambda \underline{g}^\Lambda \Big|_5^{DI} + \Big[\underline{g}_r \cdot [\, \tfrac{1}{2}(\underline{\mathcal{E}}\big|_1^{DI} + \underline{\mathcal{E}}\big|_2^{DI})] \cdot \underline{g}_r \Big] \underline{g}^r \underline{g}^r \Big|_5^{DI}$$

$$+ \Big[\underline{g}_r \cdot [\, \tfrac{1}{2}(\underline{\mathcal{E}}\big|_1^{DI} + \underline{\mathcal{E}}\big|_2^{DI})] \cdot \underline{g}_\Lambda \Big] (\underline{g}^r \underline{g}^\Lambda + \underline{g}^\Lambda \underline{g}^r)\Big|_5^{DI} \tag{11.a}$$

The strain tensor at any point inside the element is:

$$\underline{\mathcal{E}} = \underset{\text{\underline{\hspace{4cm}}}}{\tilde{\mathcal{E}}_{rr}\,\underline{g}^r\underline{g}^r + \tilde{\mathcal{E}}_{\Lambda\Lambda}\,\underline{g}^\Lambda\underline{g}^\Lambda + \tilde{\mathcal{E}}_{r\Lambda}(\underline{g}^r\underline{g}^\Lambda+\underline{g}^\Lambda\underline{g}^r)}$$
$$\text{in-layer strains} \tag{8}$$

$$+\underset{\text{\underline{\hspace{6cm}}}}{\tilde{\mathcal{E}}_{rt}(\underline{g}^r\underline{g}^t+\underline{g}^t\underline{g}^r) + \tilde{\mathcal{E}}_{\Lambda t}(\underline{g}^\Lambda\underline{g}^t+\underline{g}^t\underline{g}^\Lambda)}$$
$$\text{transverse shear strains}$$

It must be taken into account that the hypothesis of constant thickness along the director vectors, on which the element is constructed, implies $\tilde{\mathcal{E}}_{tt}=0$ [4,5].

The appropiate interpolation of the in-layer strains and of the transverse shear strains to satisfy our shell element requirements as closely as possible is the key aspect of our formulation.

To have no spurious zero energy modes, pass the patch test and avoid locking we use the following interpolations:

. In-layer strains, (see Fig. 8-c)

$$\underline{\mathcal{E}} = \sum_{i=1}^{8} h_i^{IS}\,\underline{\mathcal{E}}\Big|_i \tag{9}$$

where the h_i^{IS} are obtained from the usual serendipitic interpolation functions of the 8-node element [17, Fig. 5.5], by replacing the variable r with r/a, and the variable Λ with Λ/a ; $a = 1/\sqrt{3}$.

Also, we have for i = 1, 2, 3, 4

$$\underline{\mathcal{E}}\Big|_i = \tilde{\mathcal{E}}_{rr}\,\underline{g}^r\underline{g}^r\Big|_i^{DI} + \tilde{\mathcal{E}}_{\Lambda\Lambda}\,\underline{g}^\Lambda\underline{g}^\Lambda\Big|_i^{DI} + \tilde{\mathcal{E}}_{r\Lambda}(\underline{g}^r\underline{g}^\Lambda+\underline{g}^\Lambda\underline{g}^r)\Big|_i^{DI} \tag{10}$$

For i = 5 and 7

$$\underline{\mathcal{E}}\Big|_5 = \tilde{\mathcal{E}}_{\Lambda\Lambda}\,\underline{g}^\Lambda\underline{g}^\Lambda\Big|_5^{DI} + \left[\underline{g}_r\cdot\left[\tfrac{1}{2}(\underline{\mathcal{E}}\Big|_1^{DI}+\underline{\mathcal{E}}\Big|_4^{DI})\right]\cdot\underline{g}_r\right]\underline{g}^r\underline{g}^r\Big|_5^{DI}$$
$$+\left[\underline{g}_r\cdot\left[\tfrac{1}{2}(\underline{\mathcal{E}}\Big|_1^{DI}+\underline{\mathcal{E}}\Big|_4^{DI})\right]\cdot\underline{g}_\Lambda\right](\underline{g}^r\underline{g}^\Lambda+\underline{g}^\Lambda\underline{g}^r)\Big|_5^{DI} \tag{11.a}$$

. Transverse shear strains, (see Fig. 8-d and e)

$$\tilde{\mathcal{E}}_{rt}\ \underline{g}^r\underline{g}^t = \sum_{i=1}^{4}\ h_i^{RT}\ \tilde{\mathcal{E}}_{rt}\ \underline{g}^r\underline{g}^t\Big|_i^{DI}$$

$$+ h_5^{RT}\ [\ 1/2\ (\tilde{\mathcal{E}}_{rt}\big|_{RA}^{DI} + \tilde{\mathcal{E}}_{rt}\big|_{RB}^{DI}\ )\ ]\underline{g}^r\underline{g}^t\Big|_5^{DI} \qquad (13.a)$$

where, $h_1^{RT} = 1/4\ (1+r/a)\ (1+\Delta)\ -\ 1/4\ h_5^{RT}$

$h_2^{RT} = 1/4\ (1-r/a)(1+\Delta)\ -\ 1/4\ h_5^{RT}$

$h_3^{RT} = 1/4\ (1-r/a)(1-\Delta)\ -\ 1/4\ h_5^{RT}$

$h_4^{RT} = 1/4\ (1+r/a)(1-\Delta)\ -\ 1/4\ h_5^{RT}$ $\qquad (13.b)$

$h_5^{RT} = (1-(r/a)^2)\ (1-\Delta^2)\qquad ; \ a = 1/\sqrt{3}$

Similarly, we use

$$\tilde{\mathcal{E}}_{st}\ \underline{g}^s\underline{g}^t = \sum_{i=1}^{4}\ h_i^{ST}\ \tilde{\mathcal{E}}_{st}\ \underline{g}^s\underline{g}^t\Big|_i^{DI}$$

$$+ h_5^{ST}\ [\ 1/2\ (\tilde{\mathcal{E}}_{st}\big|_{SA}^{DI} + \tilde{\mathcal{E}}_{st}\big|_{SB}^{DI}\ )]\underline{g}^s\underline{g}^t\Big|_5^{DI} \quad (14.a)$$

where, $h_1^{ST} = 1/4\ (1+r)\ (1+\Delta/a)\ -\ 1/4\ h_5^{ST}$

$h_2^{ST} = 1/4\ (1-r)\ (1+\Delta/a)\ -\ 1/4\ h_5^{ST}$

$h_3^{ST} = 1/4\ (1-r)\ (1-\Delta/a)\ -\ 1/4\ h_5^{ST}$

$h_4^{ST} = 1/4\ (1+r)\ (1-\Delta/a)\ -\ 1/4\ h_5^{ST}$ $\qquad (14.b)$

$h_5^{ST} = (1-(\Delta/a)^2)(1-r^2)\qquad ; \ a = 1/\sqrt{3}$

Equations (13) and (14) corresponds to an interpolation of tensor components such that the bending patch test is passed (no shear locking); without introducing spurious zero energy modes.

The following observations can be made about the element:

. The presented element is a general nonlinear shell element (the total lagrangian formulation [17] was used in its implementation), with the only restriction of small strains. Linear shell elements and plate elements can be obtained as particular cases.

.The element does not lock, does not contain spurious zero energy modes and is quite insensitive to elements distortions.

. Gauss integration is used to evaluate the element matrices, 3 x 3 integration is used in the mid-surface of the element, for linear elastic material 2 points are used through the thickness, in plate elements the integration through the thickness can be analitically performed.

For nonlinear material models accuracy considerations may lead to the use of more integration points.

4.2 Verification of the shell element

4.2.1 The patch test

As we did in our MITC4 element, we begin by verifying that our 8-node element passes the different patch tests.

The patch tests shown in Fig. 9 are all passed exactly.

However, relatively small errors in displacements and stresses arise when the element sides are curved or when the mid-side nodes are not centered.

4.2.2 Some numerical experimentation

In [7] we presented an organized numerical investigation of the element, showing that,

I. The element does not have spurious zero energy modes and passes the patch test (under the above mentioned restrictions).

II. The element does not lock.

III. The element has good convergence in the usual benchmark problems, and is quite insensitive to element distortions.

IV. The element has good behavior in the nonlinear range.

In this communication we will only show a few results to illustrate on the behavior of our element, MITC8 (for mixed interpolation of tensorial components with 8 nodes).

In Fig. 10 we show the analysis of a plate with a hole in plane stress to illustrate the difference in stress prediction between the MITC8 element and the usual isoparametric plane stress element.

For the stress calculations no extrapolation or stress smoothing has been used.

The 8-node isoparametric elements yields a slightly more accurate solution; we must remember that this element passes the membrane patch test for any geometrical configuration.

In Fig. 11 we analyse again a curved cantilever, using non-distorted and distorted MITC8 elements, showing that with our element there is no locking present.
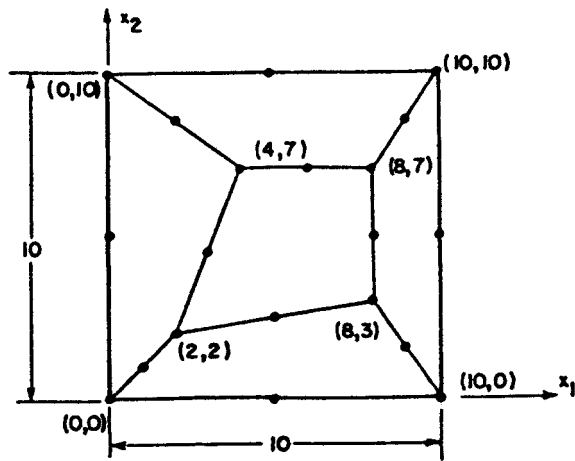
$E = 2.1 \cdot 10^6$

$\nu = 0.3$

thickness = 0.01

PATCH OF ELEMENTS CONSIDERED
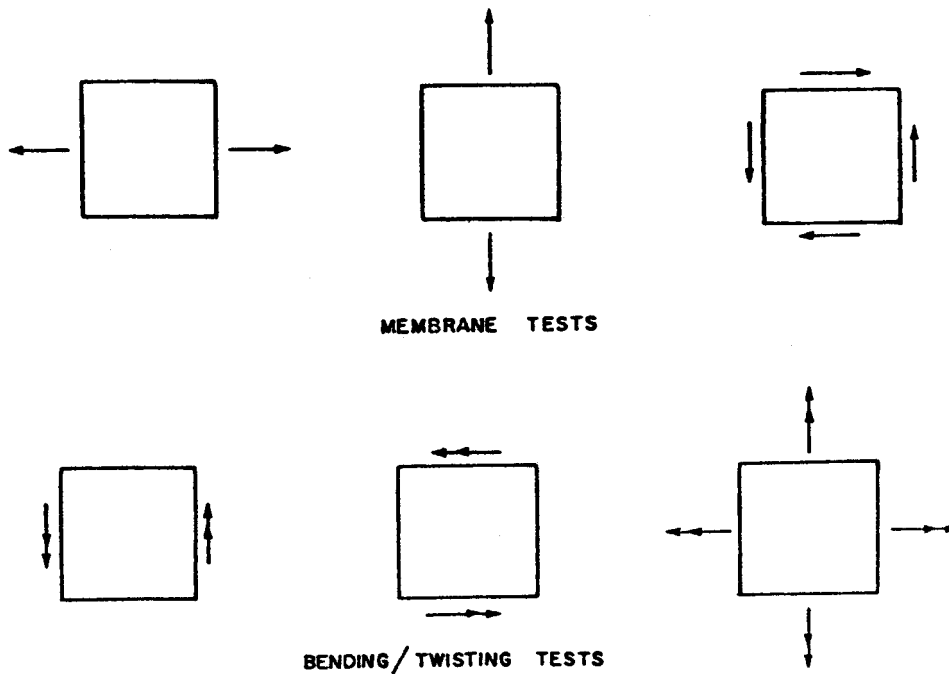
MEMBRANE TESTS

BENDING / TWISTING TESTS

Figure 9   Patch tests; for the 8-node element

In Fig. 12 we analyse the pinched cylinder problem [27] using undistorted and distorted meshes.

The figure indicates the low sensitivity of the solution results to some mesh distortions.

In Fig. 13 we analyse another benchmark problem, the Scordelis - Lo shell [28].

Finally in Fig. 14 we analyse a cantilever in large deflections/ rotations.

We observe that when using only one element to model the cantilever excellent results are obtained for up to about ninety degrees rotations.

The standard Ahmad element with "full" integration (3 x 3 x 2), which matches the exact result in linear analysis, locks in the large displacement solution.

5. SOME PRACTICAL CONSIDERATIONS

In our formulation we use the five "natural" degrees of freedom per node: three incremental displacements and two rotations of the node director vector about two axis normal to it [3,17].

Many times, due to the intersection of shells at an angle, or the intersection of beams and shells (stiffened shells) it is necessary to use six degrees of freedom at a node. We do that by transforming the five original degrees of freedom into six, but without recurring to the extended practice of adding on "artificial rotational spring" in the direction of the rotation about the director vector.

We do not add the artificial spring because in nonlinear analysis, according to our experience, it may result in artificial buckling loads and may inhibit the effective use of an automatic load stepping algo - rithm.

This means that the computer program with the shell element should allow a shell node to have either five or six degrees of freedom: the five natural degrees of freedom are used when the shell model contains only stiffness corresponding to these five degrees of freedom and no globally aligned rotational boundary conditions are imposed; otherwise the five degrees of freedom are transformed to the six global degrees of freedom, so that the element can connect to other types of elements, appropiate boundary conditions can be imposed and so on.

6. CONCLUDING REMARKS

In this communication we began by stating our requirements for a general nonlinear shell element to be a reliable tool for practical engineering analysis.

Then we reviewed our approach to meet those requirements: the mixed interpolation of tensorial components, and we examined two elements formulated using this approach.
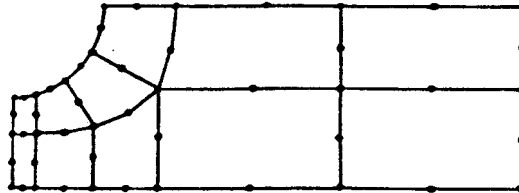
L = 56   E = 7· 10^4

b = 20 ν = 0.25

d = 10   p = 25
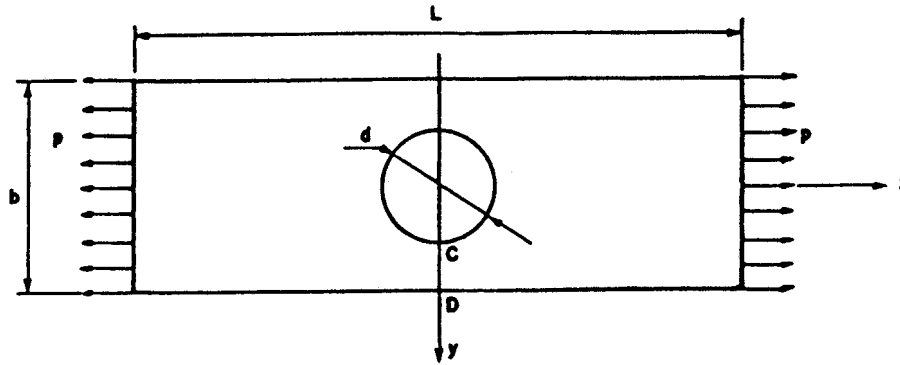
h(thickness) = 1

MESH USED

CALCULATED AT POINT	$\tau_{zz}^{FEM} / \tau_{zz}^{ANALYT.}$	
	ISOP. ELEMENT 3 X 3 X 2 INTEGRN.	MITC8
C	0.953	0.943
D	1.013	1.038

Figure 10 Analysis-of a plate with a hole in plane stress using the MITC8 element. The stresses are directly calculated at points C and D.

The 4-node element (MITC4) is effective and reliable and can be used to analyse very complex shell situations.

The 8-node element (MITC8) is also quite attractive. Further ana lysis and testing of this element is still necessary, and some refinements are desirable, specifically regarding the satisfaction of the patch tests under any distorted configuration.

As we stated above, we constructed the MITC8 element based on accumulated insight into element behavior and the patch test. It would be very valuable to place the approach on more structured mathematical foundation.

Also analytical integration through the thickness should be studied for general shell elements with linear elastic materials, to make them more effective.
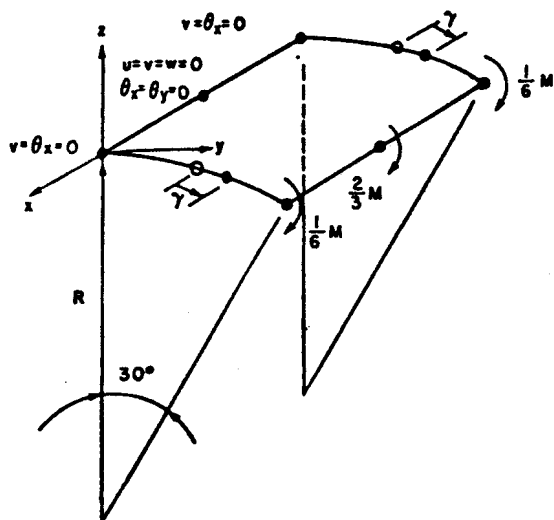
$v = \theta_x = 0$

$u = v = w = 0$
$\theta_x = \theta_y = 0$

$v = \theta_x = 0$

z

y

x

$\frac{1}{6}$ M

$\frac{2}{3}$ M

$\frac{1}{6}$ M

R

α

R = 20
h (thickness) = 0.2
E = 2.1 · 10⁶
ν = 0.3
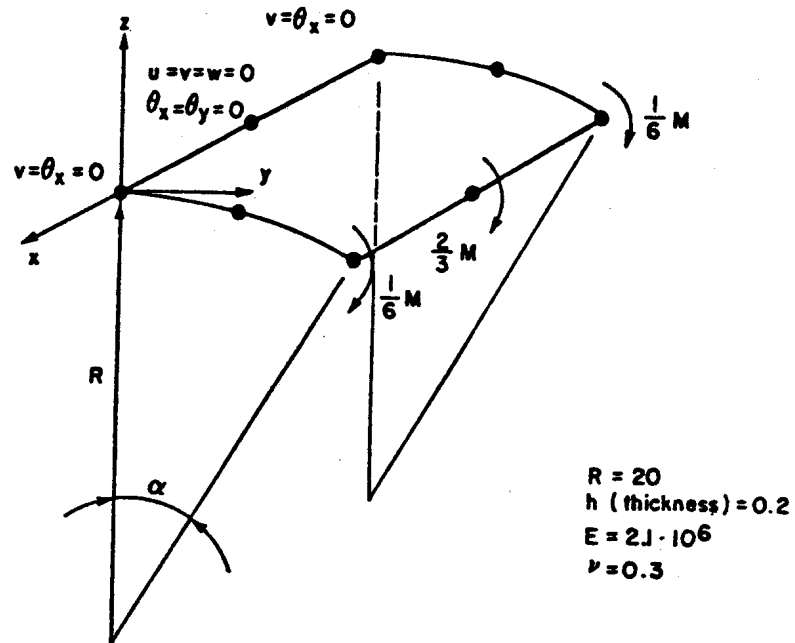
α [DEGREES]	$\theta^{FEM}/\theta^{ANALYT.}$
30	0.999
60	0.994
90	0.981

a) Results using undistorted element

Figure 11 Analysis of a curved cantilever subjected to a constant bending
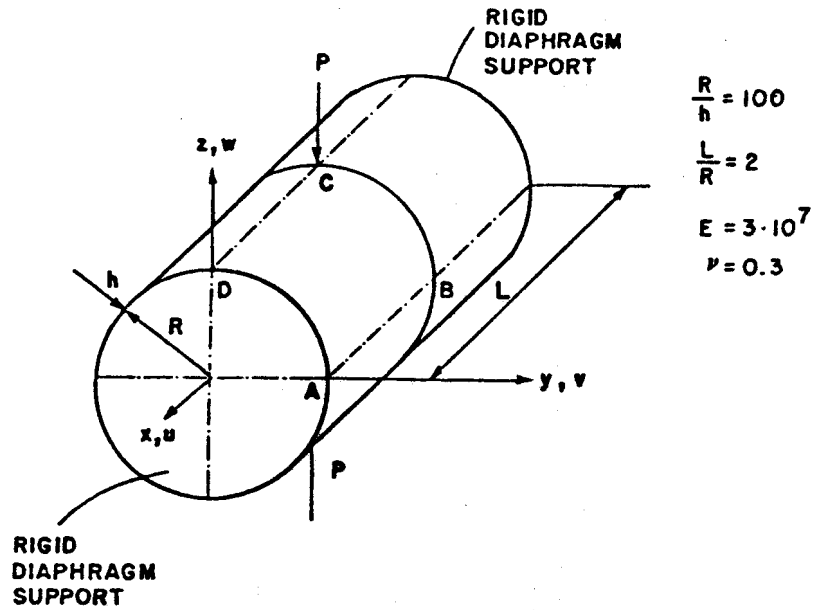moment using one MITC8 element.

γ [DEGREES]	$\theta^{FEM} / \theta^{ANALYT.}$
0	0.999
3	1.000
5	1.001
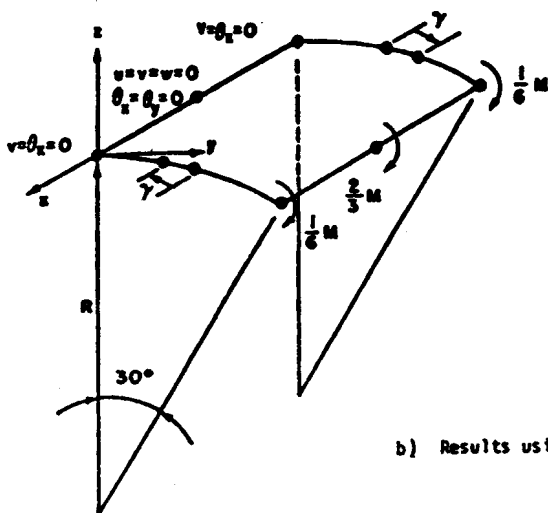
γ [DEGREES]	$\theta^{FEM} / \theta^{ANALYT.}$
0	0.999
3	0.974
5	0.928

b) Results using distorted elements

Figure 11   continued

$$\frac{R}{h} = 100$$

$$\frac{L}{R} = 2$$

$$E = 3 \cdot 10^7$$

$$\nu = 0.3$$

MESH FOR ABCD	$w_C^{FEM} / w_C^{ANALYT.}$
3 X 3	0. 833
5 X 5	0.952
8 X 8	0.990
10 X 10	0.999

a) Results using undistorted elements

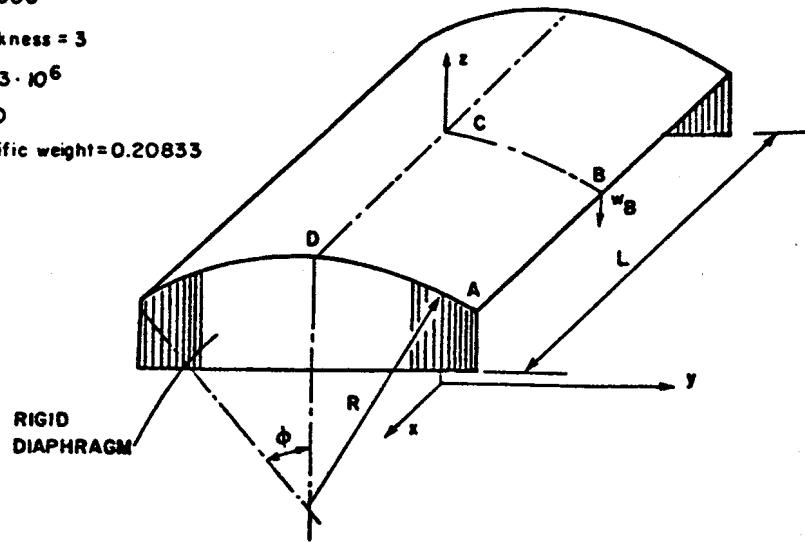Figure 12 Analysis of a pinched cylinder using the MITC8 element.
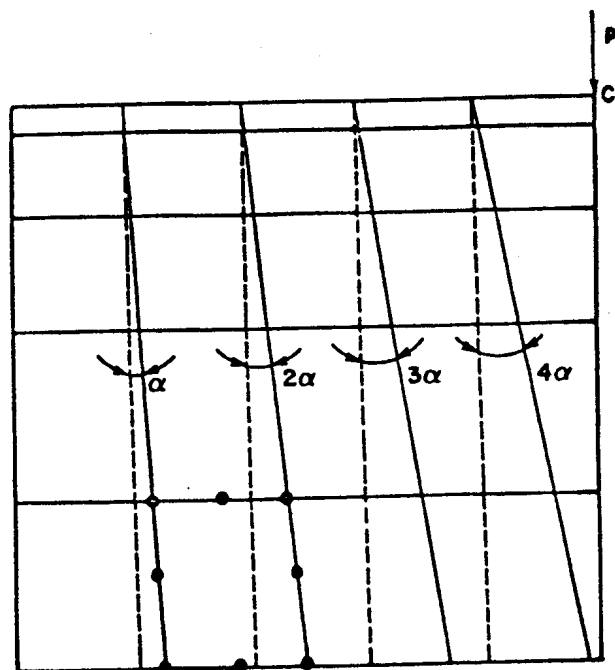
α [DEGREES]	$w_C^{FEM} / w_C^{ANALYT.}$
0	0.952
1	0.951
$1\frac{1}{2}$	0.950
2	0.949
$2\frac{1}{2}$	0.949

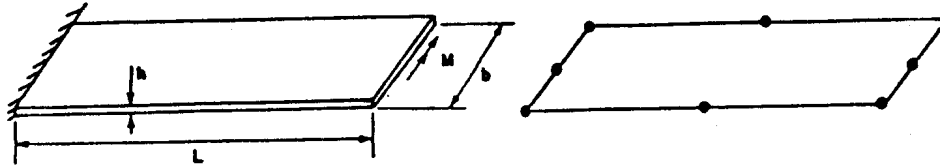b) Results using distorted elements (5 x 5 mesh)

Figure 12 continued

R = 300

L = 600

thickness = 3

$E = 3 \cdot 10^6$

$\nu = 0$

specific weight = 0.20833

RIGID
DIAPHRAGM

MESH FOR AREA ABCD	FEM w_B
2 X 2	3.48
4 X 4	3.65
6 X 6	3.63

ANALYTICAL SOLUTION w_B = 3.6
(DEEP SHELL THEORY)

Figure 13   Analysis of the Scordelis-Lo shell
using the MITC8 element.

L = 12   E = 1800   ONE 8- NODE ELEMENT MODEL

b = 1   ν = 0

h = 1

ANALYT. SOLN.

MITC8

STANDARD
ISOPARAMETRIC ELEMENT
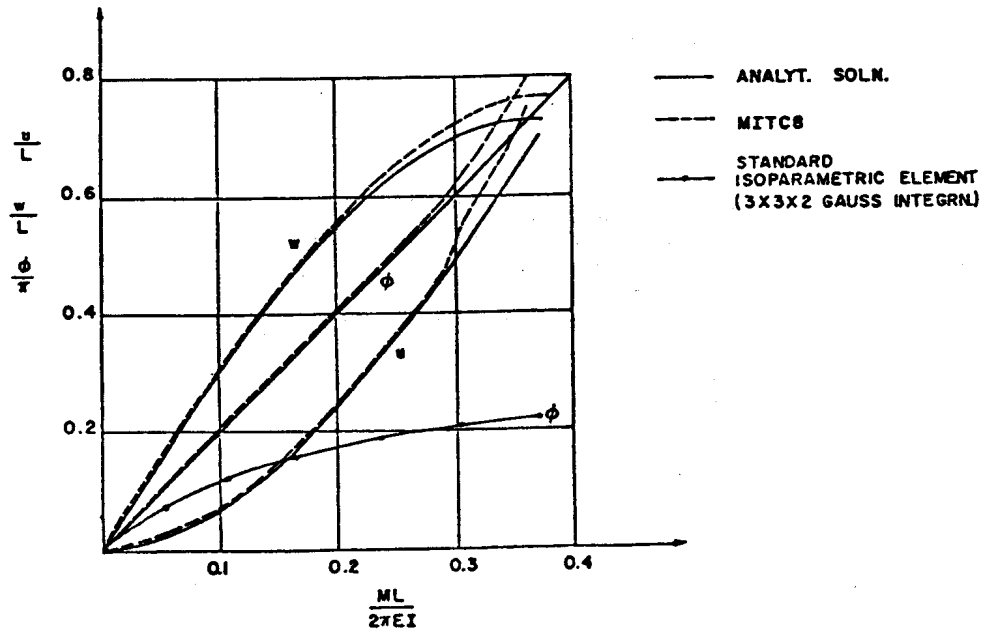(3 X 3 X 2 GAUSS INTEGRN.)

$\frac{ML}{2\pi EI}$

Figure 14 Large displacement/rotation analysis of a cantilever
using the MITC8 element.

REFERENCES

1. O.C. Zienkiewicz, The Finite Element Method (3rd Edition), McGraw-Hill, 1977.

2. K.J. Bathe and L.W. Ho, "Some Results in the Analysis of Thin Shell Structures", Nonlinear Finite Element Analysis in Structural Mechanics, (edited by W. Wunderlich et al), Springer-Verlag, Berlin, 1981.

3. K.J. Bathe and S. Bolourchi, "A Geometric and Material Nonlinear Plate and Shell Element", J. Computers and Structures, Vol 11, pp. 23-48, 1979.

4. E.N. Dvorkin, "On Nonlinear Finite Element Analysis of Shell Structures", Ph. D. Thesis, Dep. of Mechanical Eng., Massachusetts Institute of Technology, 1984.

5. E.N. Dvorkin and K.J. Bathe, "A Continuum Mechanics Based Four-Node Shell Element for General Nonlinear Analysis", Eng. Comput., Vol. 1. pp. 77-88, 1984.

6. K.J. Bathe and E.N. Dvorkin, "A Four-Node Plate Bending Element Based on Mindlin/Reissner Plate Theory and a Mixed Interpolation", Int. J. Numerical Meth. Eng., Vol. 21, pp. 367-383, 1985.

7. K.J. Bathe and E.N. Dvorkin, "A Formulation of General Shell Elements - the Use of Mixed Interpolation of Tensorial Components", Int. J. Numerical Meth. Eng., to appear.

8. K.J. Bathe, E.N. Dvorkin, and L.W. Ho, "Our Discrete-Kirchhoff and Isoparametric Shell Elements for Nonlinear Analysis - An Assessment", J. Computers and Structures, Vol. 16, pp. 89-98, 1983.

9. B. Irons and S. Ahmad, Techniques of Finite Elements, Ellis Harwood Ltd., 1980.

10. K. Washizu, Variational Methods in Elasticity & Plasticity, (3rd Edition), Pergamon Press, 1982.

11. K.J. Bathe and F. Brezzi, "On the Convergence of a Four-Node Plate Bending Element Based on Mindlin/Reissner Plate Theory and a Mixed Interpolation", Proceedings Conference on Mathematics of Finite Elements and Applications V, Brunel University, England, 1984.

12. H.C. Huang and E. Hinton, "A Nine Node Lagrangian Mindlin Plate Element with Enhanced Shear Interpolation", Eng. Comput., Vol. 1, pp. 369-379, 1984.

13. M.A. Crisfield, "A Quadratic Mindlin Element Using Shear Constraints", J. Computers and Structures, Vol. 18, pp. 833-852, 1984.

14. K.C. Park and G.M. Stanley, "A Curved C° Shell Element Based on Assumed Natural-Coordinate Strains" Report N° LMSC-F035235, Applied Mechs. Lab., Lockheed Palo Alto Research Lab., 1984.

15. S. Ahmad, B.M. Irons, and O.C. Zienkiewicz, "Analysis of Thick and Thin Shell Structures by Curved Finite Elements", Int. J. Numerical Meth. Eng., Vol. 2, pp. 419-451, 1970.

16. E. Ramm, "A Plate/Shell Element for Large Deflections and Rotations", Formulations and Computational Algorithms in Finite Element Analysis, (edited by K.J. Bathe et al), M.I.T. Press, 1977.

17. K.J. Bathe, Finite Element Procedures in Engineering Analysis, Prentice-Hall, Englewood Cliffs, New Jersey, 1982.

18. H. Stolarski and T. Belytschko, "Membrane Locking and Reduced Integration for Curved Elements", ASME, J. Appl. Mech., Vol. 49, pp. 172-176, 1982.

19. O.C. Zienkiewicz, R.L. Taylor and J. M. Too, "Reduced Integration Technique in General Analysis of Plates and Shells", Int. J. Numerical Meth. Eng., Vol. 3, pp. 275-290, 1971.

20. R.H. MacNeal, "Derivation of Element Stiffness Matrices by Assumed Strain Distributions", J. Nuclear Eng. and Design, Vol. 70, pp. 3-12, 1982.

21. T.J.R. Hughes and T.E. Tezduyar, "Finite Elements Based upon Mindlin Plate Theory with Particular Reference to the Four-Node Bilinear Isoparametric Element", ASME, J. Appl. Mech., Vol. 46, pp. 587-596, 1981.

22. G. Wempner, D. Talaslidis and C. - M. Hwang, "A Simple and Efficient Approximation of Shells via Finite Quadrilateral Elements", ASME, J. Appl. Mech., Vol. 49 pp. 115-120, 1982.

23. G. Strang and G.J. Fix, An Analysis of the Finite Element Method, Prentice-Hall, Englewood Cliffs, New Jersey, 1973.

24. E. Reissner, "On the Transverse Twisting of Shallow Spherical Ring Caps" ASME, J. Appl. Mech., Vol. 47, pp. 101-105, 1980.

25. B. Kråkeland, "Nonlinear Analysis of Shells Using Degenerate Isoparametric Elements", Finite Elements in Nonlinear Mechanics, Vol. 1, (edited by P.G. Bergan et al), Tapir Publisher, (Norwegian Inst.of Tech. Trondheim, Norway), 1978.

26. K. J. Bathe and E. N. Dvorkin, "On the Automatic Solution of Nonlinear Finite Element Equations", J. Computers and Structures, Vol. 17, pp. 871-879, 1983.

27. G.M. Lindberg, M. D. Olson, and G.R. Cowper, "New Developments in the Finite Element Analysis of Shells", Quarterly Bulletin of the Divisions of Mech. Eng. and the National Aeronautical Establishment, National Research Council of Canada, Vol. 4, 1969.

28. K. Forsberg and R. Hartung, "An Evaluation of Finite Difference and Finite Element Techniques for Analysis of General Shells", Symposium on High Speed Computing of Elastic Structures, I.U.T.A.M., Liège, 1970.